Very high levels of misincorporated ribonucleotides increase Topoisomerase-1 related genome alterations

Lijia Zhang

A thesis submitted to the Department of Biology for honors
Department of Molecular Genetics and Microbiology
Duke University
Durham, North Carolina

May 2017

Abstract:

A combination of high-resolution mapping of genomic rearrangements throughout the genome using microarrays, and measurements of loss of heterozygosity (LOH) on the right arm of chromosome IV were used to examine the effects of misincorporated ribonucleotides (rNMPs) on genome stability in diploid *Saccharomyces cerevisiae* strains. The effects of three types of mutations were examined in my analysis. Strains with a *top1* mutation lack the Topoisomerase 1 enzyme, an enzyme that is involved in relaxing supercoils and in the removal of rNMPs from the genome. Strains with the *rnh201* mutation lack RNase H2, an enzyme that removes both R-loops (RNA-DNA hybrids formed during transcription) and misincorporated rNMPs. Lastly, strains with the *pol2-M644G* mutation have a mutant form of DNA polymerase ε that misincorporates about 10-fold more rNMPs than the wild-type enzyme. My analysis of genetic instability in single mutants and various combinations of double and triple mutants shows that high levels of misincorporated rNMPs elevate mitotic recombination. Since mitotic recombination events are initiated in yeast by double-stranded DNA breaks (DSBs), my results suggest that high levels of misincorporated rNMPs result in elevated levels of DNA breaks.

Introduction:

Although the genomes of wild-type cells are generally quite stable, various mutations can substantially elevate genetic instability. These alterations include point mutations, chromosomal translocations, deletions/ duplications, and changes in ploidy (loss or gain of a whole chromosome). Some of these alterations can induce double-stranded DNA breaks (DSBs), which in yeast, is usually repaired by homologous recombination. In diploids in which the two homologs contain single-nucleotide polymorphisms (SNPs), mitotic crossovers can be detected by loss of heterozygosity (LOH) of SNPs that were originally heterozygous. In addition to crossovers, which cause LOH for all SNPs distal to the crossover, repair of a DSB can result in non-reciprocal LOH region (gene conversion). Although some genomic alterations may be beneficial to the cell or organism because they produce new variants that can be acted on by evolutionary forces, such alterations are also associated in higher organisms with increased cancer susceptibility and developmental disorders (Motegi & Myung, 2007). There is evidence that mutations in DNA repair and checkpoint genes predispose the development of human cancers (Aguilera & Gómez González, 2007).

The DSBs that occur in wild-type and mutant cells are likely the consequence of a variety of types of DNA damage. Some DNA lesions may be introduced as a consequence of faulty DNA repair pathways (base excision repair, nucleotide excision repair, mismatch repair) or mistakes made during DNA replication. My thesis will be concerned with genetic instability related to interactions of RNA and DNA. Two types of RNA-DNA interactions are relevant: DNA breaks associated with the formation of RNA-DNA hybrids (R-loops) and DNA damage associated with misincorporated rNMPs. Each of these two types of recombinogenic lesions will be discussed below.

Recent research has identified transcription, specifically lesions generated by RNA:DNA hybrids, as another cause of genetic instability (Huertas & Aguilera, 2003; Gaillard & Aguilera, 2016). R-loops are formed transiently during transcription, but can also form as a consequence of a re-invasion of the RNA molecule into the duplex (Gaillard & Aguilera, 2016). The evidence that R-loops contribute to genetic instability is based on several types of experiments. First, high levels of transcription stimulate mitotic recombination in yeast (Keil & Roeder, 1984). Second, some hyper-Rec mutants result in elevated R-loop formation (Gaillard & Aguilera, 2016). It should also be noted that mutations affecting the accumulation of RNA:DNA hybrids result in the diseases Aicardi-Goutiéres syndrome and systemic lupus erythematosus (Crow *et al.*, 2006; Günther *et al.*, 2015). The mechanism by which RNA-DNA hybrids stimulate recombination is not completely clear. It has been suggested that these hybrids may block replication forks, leading to subsequent DSBs. Alteratively or in addition, the hybrids may attract DNA repair enzymes that generate single-stranded nicks or DSBs (Gaillard & Aguilera, 2016).

A second type of RNA-related recombinogenic lesion is misincorporated ribonucleotides. Although DNA polymerase has a strong bias for the insertion of deoxyribonucleotides, in *Saccharomyces cerevisisiae*, ribonucleotide triphosphate concentrations are much higher than the concentration of deoxyribonucleoside triphosphates. Approximately 15,000 ribonucleotides (rNMPs) are misincorporated into the genome with every cell division (Williams & Kunkel, 2014). Ribonucleotides, when inserted into the genome during replication either by direct incorporation or as Okazaki fragment remnants, can also lead to genetic instability (Williams & Kunkel, 2014).

The evidence that such rNMPs result in elevated genomic instability is based on measurements of instability in strains with mutations that have either elevated or reduced levels

of misincorporation. Levels of rNMPs can be modulated with DNA polymerase ε (Pol ε) variants. Of the three DNA polymerases that are active during DNA replication (α, δ, and ε), polymerase ε is the primary polymerase involved in replicating the leading strand. Past research has shown that genomic instability related to rNMP incorporation is primarily caused by rNMPs inserted by Pol ε, compared to Pol α and Pol δ (Williams *et al*., 2015). Certain amino acids at DNA polymerase active sites act as "steric gates" in order to block rNMP insertion (Joyce, 1997). In yeast, replacement of a methionine residue near this gate (Met644) affects the incorporation of rNMPs. The replacement of methionine with glycine (*pol2-M644G*) increases rNMP insertion levels by 11-fold whereas replacement of methionine with leucine (*pol2-M644L*) decreases rNMP insertion levels by 3-fold (McElhinny *et al.*, 2010). As will be discussed further below, elevated and reduced levels of rNMPs result in elevated and reduced levels, respectively, of genome instability in some genetic assays (Conover *et al.*, 2015). Although misincorporated rNMPs likely cause genetic instability by several different mechanisms, one pathway involves topoisomerase I. In strains with rNMP-associated instability, mutations in the *TOP1* gene reduce the level of instability (Potenski *et al.*, 2014). It was suggested that Top1-generated removal of rNMPs from genomic DNA produced recombinogenic DNA lesions.

The levels of both RNA-DNA hybrids and misincorporated rNMPs are regulated, in part, by two RNase H activities, RNase H1 and RNase H2. The activities of RNase H1 and RNase H2 are somewhat functionally redundant in the removal of RNA-DNA hybrids with both enzymes being capable of degrading the RNA component of hybrids (Costantino & Koshland, 2015). RNase H2, but not RNase H1, can also remove rNMPs embedded in the genome in a relatively error-free manner (Cerritelli & Crouch, 2009). RNase H1 is encoded by the *RNH1* gene, whereas RNase H2 is a trimeric protein of which the catalytic subunit is encoded by *RNH201*.

Two recent studies have examined the roles of the RNase H proteins on genetic instability in yeast and have reached somewhat different conclusions. In the study of O'Connell *et al.* (2015), genomic instability was examined in diploids of six different genotypes: wild-type, *pol2-M644L*, *rnh1*, *rnh201*, *rnh201 pol-M644L*, and *rnh1 rnh201*. The *rnh201* strain, expected to have elevated levels of both R-loops and misincorporated rNMPs, had a high rate of genomic instability. Thus, either type of RNA-associated lesion could contribute to the instability. To distinguish which lesion was most important, O'Connell *et al.* (2015) measured the level of genome instability in the double mutant *rnh201 pol2-M644L* strain. Since *pol2-M644L* reduces the level of rNMPs by about three-fold, the double mutant strain should have a three-fold reduction in instability if the rNMPs are the primary recombinogenic lesion. Since only a slight (about 25%) reduction was observed, O'Connell *et al.* (2015) concluded that R-loops rather than rNMPs were the primary recombinogenic lesion.

In contrast, using somewhat different assays for genome instability, Conover *et al.* (2015) concluded that rNMPs, rather than R-loops, were responsible for genome instability. Their conclusion was based primarily on the observation that a double mutant *pol2-M644G rnh201* strain had substantially more instability (about three-fold) than a strain with only the *rnh201* mutation. Since *pol2-M644G* elevates the frequency of misincorporated rNMPs about eleven-fold, but is not known to affect the level of R-loops, Conover *et al.* (2015) interpreted this result as indicating that rNMPs were the primary recombinogenic lesion.

In the O'Connell *et al.* (2015) and Conover *et al.* (2015) studies, different assays for genome instability were used. In my thesis (described below), I used the same three assays of genetic stability used by O'Connell *et al.* (2015) to examine three new relevant strains: *pol2-M644G*, *rnh201 pol2-M644G*, and *rnh201 pol2-M644G top1*. My conclusion is that rNMPs are

recombinogenic in mutants with very high levels of rNMPs, but in strains with low levels of rNMPs, R-loops are likely the relevant recombinogenic DNA lesion.

Materials and Methods:

Strain Construction

In constructing the strains used in the experiment, we used derivatives of the sequence-diverged haploid strains W303-1A and YJM789. These haploids were genetically altered by transformation with PCR-generated DNA fragments or obtained through sporulation of other diploid strains. Spore genotypes were confirmed by screening for their auxotrophic markers via replica-plating onto omission media. The modified W303-1A and YJM789 haploids were then crossed to generate the desired diploids used in this study. The polymerase chain reaction (PCR) was used to determine the mating type of the W303-1A and YJM789 haploids; mating only occurs with the combination of opposite mating types (*MATa* and *MATα*). The constructed strains were confirmed by screening for auxotrophic and drug-resistance markers by a combination of replica-plating and PCR. The three diploids used for most of my analysis are listed in Table S1, and various strains used in the construction of these diploids are listed in Table S2.

Rate of crossovers on the right arm of chromosome IV as determined by measuring the frequency of red/white sectored colonies

As described in the text, the frequency of red/white sectors in our diploids allows an estimate of the rate of mitotic crossovers on the right arm of chromosome IV. The diploid strains were constructed with one copy of IV having a *URA3* gene from *Kluyveromyces lactis* (*URA3-Kl*) inserted near the right telomere on the W303-1A-derived homology and an *ADE2* gene at the allelic position on the YJM789-derived homolog (Fig. 1). For these experiments, dilutions of the diploid strain were plated on rich growth medium (YPD) as a concentration of about 1000

cells/plate. After incubating for 2-3 days at 30^0, the plates were screened under a dissecting microscope for red/white sectors; the starting diploid forms pink colonies. As shown in Fig. 1, a variety of different types of events can produce a red/white sectored colony including reciprocal crossovers (RCO; Fig. 1A, break-induced replication (BIR, Fig. 1B), and chromosome loss (Fig. 1D). In order to form a red/white sector, the crossover or BIR event must occur during the first mitotic division. Thus, the rate of red/white sector formation is the frequency of sectors divided by the total number of colonies. We then used an automated R program to obtain the respective 95% confidence intervals.

I then isolated single colonies from the red and white sectors, and streaked them onto YPD plates for subsequent genomic and phenotypic analysis. These colonies were then replica-plated onto media lacking either uracil or tryptophan. As shown in Fig. 1A, an RCO would produce red colonies that are phenotypically Ade^- Ura^+ Trp^+, and white colonies that are Ade^+ Ura^- Trp^+. A BIR event initiated by a DSB on the YJM789-derived homolog would produce red colonies that are phenotypically Ade^- Ura^+ Trp^+, and white colonies that are Ade^+ Ura^+ Trp^+ (Fig. 1B). A BIR event initiated on the W303-1A-derived homolog would not produce a red/white sectored colony (Fig. 1C). Lastly, a red/white sectored colony resulting from loss of the YJM789-derived homolog would produce red colonies that are phenotypically Ade^- Ura^+ Trp^-, and white colonies that are Ade^+ Ura^+ Trp^+ (Fig. 1D). In summary, by testing for these phenotypes, I could easily distinguish RCO, BIR, and chromosome loss as causes of red/white sectored colony formation.

Monitoring genome instability by measuring rates of 5-fluoro-orotate (5-FOA) resistance

Although our assay of genome instability by examining red/white sectored colonies is very useful, since it is a non-selective method and the rate of the events is low, I could only examine a limited number (less than 100) events per strain. As an alternative method, using the same diploid strain, I selected cells that had lost the *URA3* gene; strains that have the wild-type *URA3* gene are sensitive to the drug 5-FOA. As shown in Fig. 1, RCO or BIR events (Figs. 1A and 1C) will lead to the formation of strains that are Ura^- and, therefore, 5-FOA-resistant. In addition, loss of the W303-1A-derived homolog can produce this same phenotype. In summary, measuring the rate of 5-FOA-resistance is a general indication of genome stability, although this method does not distinguish among a number of possible genomic alterations.

To measure the rate of 5-FOA-resistance, I suspended 10-20 individual colonies per genotype in 1 mL of water each. 100 µL of each suspension were plated onto media containing 1mg/mL of 5-FOA and a dilution of the suspension was plated onto non-selective YPD plates. I then counted the number of colonies that survived on the 5-FOA plates and the total number of colonies on the YPD plates. Using those measurements, we calculated the rate of 5-FOA-resistance using the method of the median (Lea & Coulson, 1949); the 95% confidence intervals were obtained using Table B11 in Altman (1990).

Analyzing genomic instability using DNA microarrays of sub-cultured mutant strains

The third method of analysis was to use microarrays. As described below, this method allowed us to examine genomic instability throughout the genome. Since preliminary experiments indicated that the rate of genomic alterations per cell division was low, I first sub-cultured strains to allow accumulation of genetic variants. For each strain, two independently-constructed isolates were streaked with sterile toothpicks to single colony density on rich YPD

medium at 30^0. Five to ten colonies from each plate were then re-streaked, and serially passaged onto YPD either 10 or 20 times. This protocol corresponds to ~250 to ~500 cell divisions, respectively.

The microarrays used for our analysis monitor LOH at about 13,000 SNPs distributed throughout the genome, allowing the mapping of LOH events to an average resolution of about 1 kb (St. Charles *et al.*, 2012). Each SNP is represented by four 25-base oligonucleotides on the microarray, two identical to the Watson and Crick strands of the W303-1A-specific sequence and two identical to the Watson and Crick strands of the YJM789-specific sequence. If the diploid is heterozygous for the SNP, we observe about equal levels of hybridization to all four oligonucleotides. If the diploid has an LOH event in which one or more YJM789-specific SNPs are lost and W303-1A-specific SNPs are duplicated, we detect an increase in the level of hybridization to the W303-1A-specific oligonucleotides and a reduction in the level of hybridization to the YJM789-specific oligonucleotides. As discussed below, in all of the hybridization experiments, we include a differentially-labeled control DNA sample that has no LOH events.

In order to extract the DNA samples for microarray analysis, I grew the yeast cells to stationary phase in 15 mL liquid YPD cultures at 30^0. The cells were harvested by centrifugation and resuspended in a solution of 500 µL molten agarose (0.5% low-melt agarose and 100 mM EDTA) and 20 µL of zymolyase (25mg/mL concentration). The combination of cells, agarose, and zymolyase was poured into plug molds (100 µL) and allowed to solidify at 4^0 for 30 minutes. The plugs were then suspended into 1mL of TE buffer (10mM Tris/500 mM EDTA) and incubated at 37^0 for at 10-24 hours. I then added 100 µL of a 5% sarcosyl, 5 mg/ml proteinase-K in 500mM of EDTA (pH7.5) solution to the samples, incubating the samples at 50^0

for 12-24 hours. The samples were then washed twice with TE buffer and incubated on a shake table for 12-24 hours. Following this incubation, I washed the samples again with TE buffer and extracted the DNA using the methods described in St. Charles *et al.* (2012). The DNA samples were then sonicated, yielding DNA fragments of ~250 bp. The DNA concentrations were measured with a Qubit fluorometer; a minimum of 100 µg/mL of DNA was necessary for microarray analysis.

The DNA samples from the sub-cultured strains were hybridized onto our microarray slides (purchased from Agilent) in competition with control DNA samples that were heterozygous for all SNPs, following the methods detailed in St. Charles *et al.* (2012). The experimental DNA was labeled with Cy3-dUTP and the control DNA was labeled with Cy5-dUTP; both samples were combined and hybridized to the microarrays. The locations and sequences of the oligonucleotides on the microarrays are described in in St. Charles *et al.* (2012).

After hybridization, the arrays scanned with the GenePix scanner and GenePix Pro 6.1 software. Using the Batch Analysis feature in the GenePix Pro 6.1 software, I obtained a (.gpr) file that shows the "ratio of medians (635 nm/ 532 nm)" for each oligonucleotide. This ratio reflects the relative fluorescence of the Cy5-experimental to the Cy3-control sample. We then used Perl and R programs to analyze, normalize, and plot the hybridization levels through the genome. Hybridization ratios of heterozygous SNPs for the samples were ~1 to both the W303-1A- and YJM789-specific oligonucleotides. In LOH regions, the ratio of hybridization of one background would be ~1.5 and the other at ~0.2. We then categorized the patterns of LOH into terminal LOH, interstitial LOH, aneuploidy, and deletions/ duplications. Frequencies of these classes of events were then recorded in Microsoft Excel.

Results

I used three different systems to monitor genome stability (details of the assays in Materials and Methods). Below, I will describe the results obtained with each assay. In general, the results of the tests were in good agreement.

Measurements of crossovers, break-induced recombination events, and chromosome loss using the red/white sectored colony assay in pol2-M644G, rnh201 pol2-M644G, and rnh201 pol2-M644G top1 strains

In all three of the mutant strains used in my study, the diploids were heterozygous for an insertion of the *ADE2* gene located near the right end of chromosome IV (YJM789-derived homolog), and had a *URA3* gene at the allelic position on the W303-1A-derived homolog (Fig. 1). In addition, in all strains, the YJM789-derived homolog has a wild-type *TRP1* gene. Loss of *ADE2* results in a derivative in which a red precursor to adenine accumulates. Thus, if a cell loses the *ADE2* marker by one of the events shown in Figs. 1A, 1B, or 1D, a red/white sectored colony would be formed. The phenotypes (Ura^+ or Ura^-, Trp^+ or Trp^-) for the red and white sectors are different for the events shown in Figs. 1A, 1B, and 1D, and I used replica-plating to classify each sectored colony.

Before discussing the data, I will emphasize a few points. First, it is likely that all of the events producing a red/white sectored colony reflect the repair of DNA damage, likely the repair of a DSB. For the RCO, distal to the point of the crossover, we detect reciprocal LOH; one sector (the red) loses the *ADE2* marker and duplicates the *URA3* marker, and the other (the white) loses the *URA3* marker and duplicates the *ADE2* marker. Second, the break-induced replication (BIR) event is inherently non-reciprocal. As shown in Fig. 1B, the sequences distal to the DSB are lost

from one chromosome, and duplicated from the other. This process involves the broken end "invading" the intact homolog and copying it by DNA replication. Third, the class of BIR in which the W303-1A-derived homolog is broken does not produce a red/white sectored colony, and is not detected in my analysis. Lastly, in a previous study from the Petes lab, O'Connell *et al.* (2015) used the same three methods to examine genome stability in a wild-type strain and in an *rnh201* strain. I include these data in my thesis to allow certain important comparisons. It should be emphasized that the wild-type and *rnh201* strains are isogenic with the ones used in my analysis.

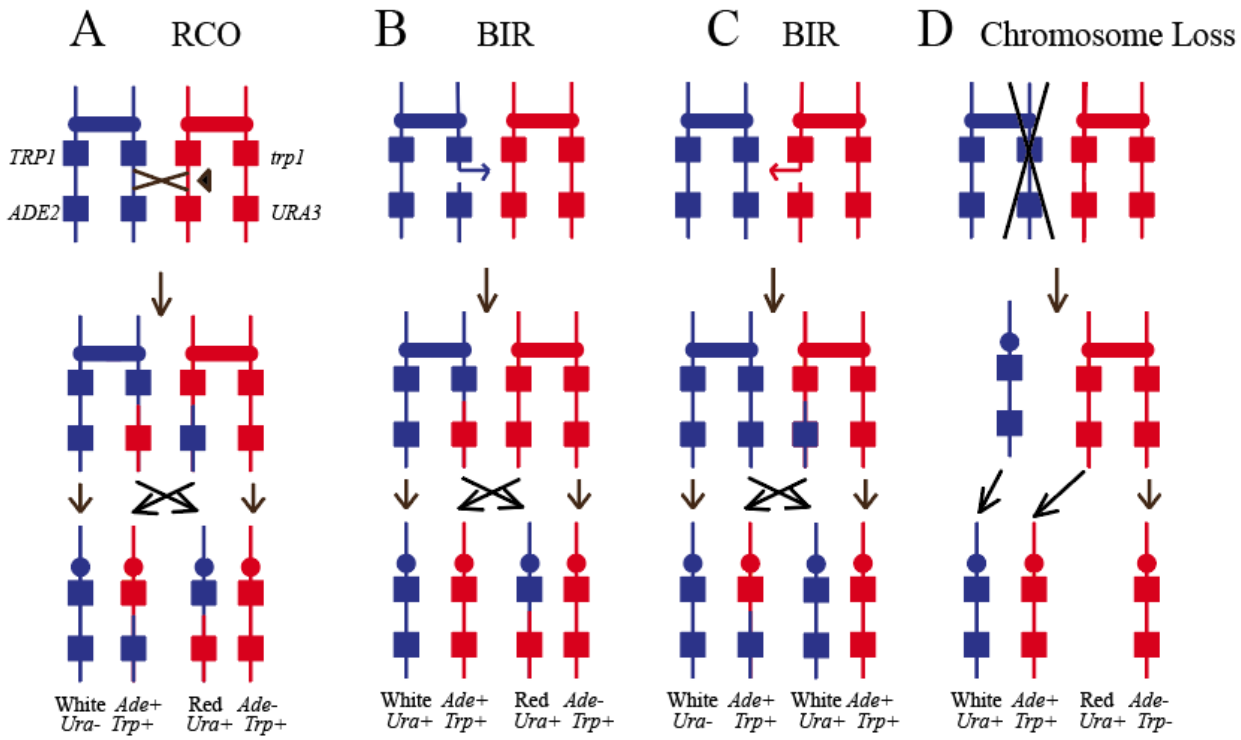

Figure 1. Mechanisms of repair leading to red/white sectored colonies and 5-FOA-resistant colonies (modified from O'Connell *et al.*, 2015). The colored chromosomes represent the W303-1A- (red) and YJM789-derived (blue) homologs. Sectors lacking the *ADE2* gene are red. (A) Reciprocal crossover (RCO). (B) Break-induced replication (BIR) in which the initiating DSB is on the YJM789-derived homolog. (C). BIR event in which the initiating DSB is on the W303-1A-derived homolog; no red/white sector is formed as the result of this event. (D). The loss of the YJM789-derived homolog.

The rates of red/white sectors (95% confidence limits in parentheses) in my analysis (separated into RCO and BIR events in brackets) were: 1.49E-04 (1.05E-04, 2.06E-04) [0 RCO, 1.49E-04 BIR] in *pol2M644G*; 1.23E-03 (9.43E-04, 1.59E-03) [7.79E-04 RCO, 4.54E-04 BIR] in *rnh201*Δ *pol2-M644G*, and 5.35E-04 (3.95E-04, 7.10E-04) [2.26E-04 RCO, 3.09E-04 BIR] in *rnh201*Δ *pol2-M644G top1*Δ. These rates are displayed in Fig. 2 along with relevant data obtained from O'Connell *et al.* (2015): sectoring rate of 1.04E-04 (5.91E-05, 1.70E-04) [8.16E-05 RCO, 2.22E-05 BIR] in wild-type, and 3.73E-04 (3.12E-04, 4.43E-04) [3.17E-04 RCO, 5.62E-05 BIR] in *rnh201*Δ.

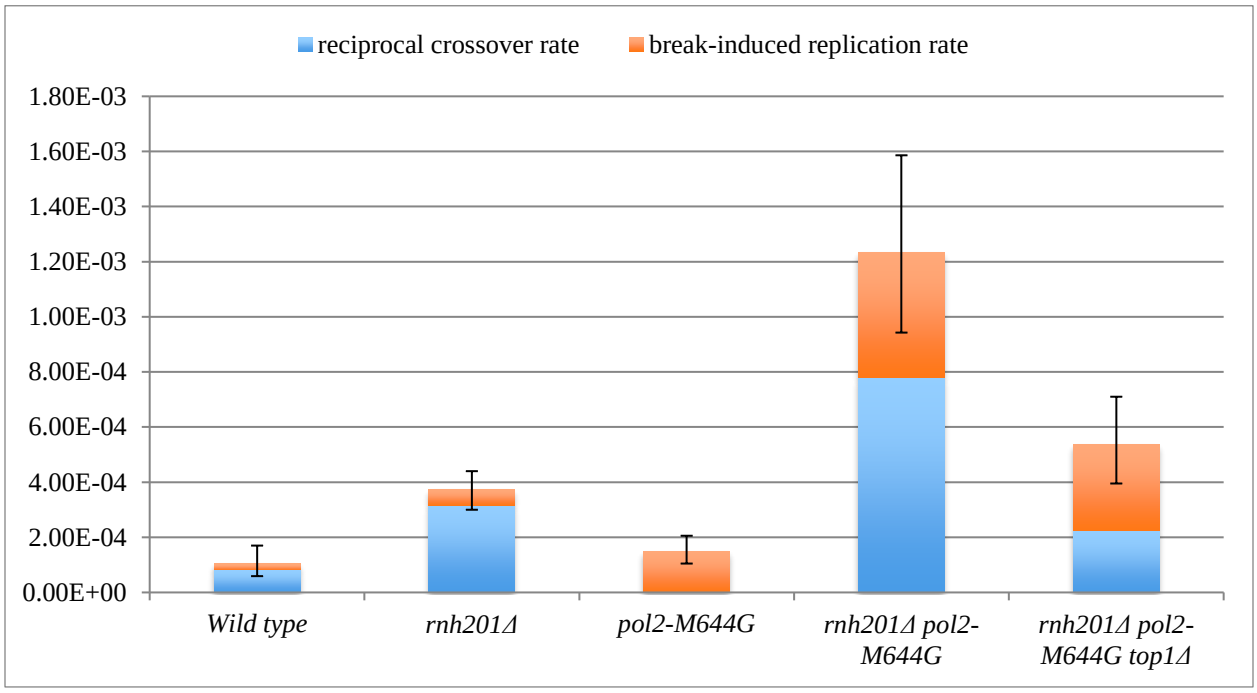

Figure 2. Red/white sectoring rates as an assay of the rates of reciprocal crossovers and BIR in wild-type and mutant strains. The rate of red/white sector formation is shown for wild type, *rnh201*Δ, *pol2-M644G*, *rnh201*Δ *pol2-M644G*, and *rnh201*Δ *pol2-M644G top1*Δ. The bars indicate the median sectoring rates with error bars representing the 95% confidence intervals. The rates of reciprocal crossover (RCO) and break-induced replication (BIR) are shown in blue and yellow, respectively.

These experiments demonstrate that strains with the *pol2-M644G* mutation (leading to 11-fold elevated levels of rNMPs) has no significant effect on the rate of red/white sectored

colonies. In contrast, the double mutant strain *rnh201Δ pol2-M644G* has a three-fold elevated rate of sectored colonies relative to the *rnh201Δ* single mutant strain, and an eight-fold elevated rate in comparison to the *pol2-M644G* single mutant. Since strains lacking Rnh201 have a reduced ability to excise rNMPs from the genome, this result suggests that high levels of rNMPs lead to genome instability. In addition, the level of instability observed in the *rnh201Δ pol2-M644G* strain is reduced about two-fold in the *rnh201Δ pol2-M644G top1Δ* strain. As will be discussed in detail, this observation indicates that the Top1 enzyme acts to remove rNMPs in a mechanism that is recombinogenic. No chromosome loss events were observed in the sectors for the *pol2-M644G* or *pol2-M644G rnh201*Δ *top1*Δ strains.

Measurements of genome instability using the 5-FOA-resistance in pol2-M644G, rnh201 pol2-M644G, and rnh201 pol2-M644G top1 strains

One disadvantage of the red/white sectoring assay is that it is non-selective. Therefore, I had to screen a very number (often >100,000) colonies to detect a limited number of sectored colonies. As shown in Fig. 1, a number of the depicted events result in a daughter cell that is Ura^-; such cells are resistant to the drug 5-fluoro-orotate (Boeke *et al*., 1984). Thus, we can select for events that lead to LOH of *URA3*. This assay leads to more accurate measurements of LOH than the red/white sectoring assay since it is based on a larger number of events. However, the assay does not distinguish between RCO and BIR events, since both classes of events result in cells that have the Ura^- Trp^+ Ade^+ phenotype. In addition, loss of the W303-1A-derived homolog would also produce cells with this same phenotype. Based on our results using the red/white sectoring assay, chromosome loss events are expected to be very infrequent relative to RCO and BIR.

The rates of formation of 5-FOA resistant derivative in my study (with 95% confidence intervals shown in parentheses) are: 1.64E-04 (1.36E-04, 1.92E-04) in *pol2M644G*, 6.61E-04 (5.66E-04, 7.54E-04) in *rnh201*Δ *pol2-M644G*, and 4.66E-04 (3.48E-04, 5.20E-04) in *rnh201*Δ *pol2-M644G top1*Δ. O'Connell et al. (2015) found rates of formation of 5-FOA-resistant strains of 4.77E-05 (3.54E-05, 6.16E-05) in wild-type and 2.66E-04 (2.52E-04, 3.96E-04) in *rnh201*Δ. These data are shown in Fig. 3. In general, these results are in broad agreement with those observed in the red/white sectoring assay, although in the 5-FOA assay, the *pol2-M644G* single mutant had a greater rate of LOH than the wild-type strain.

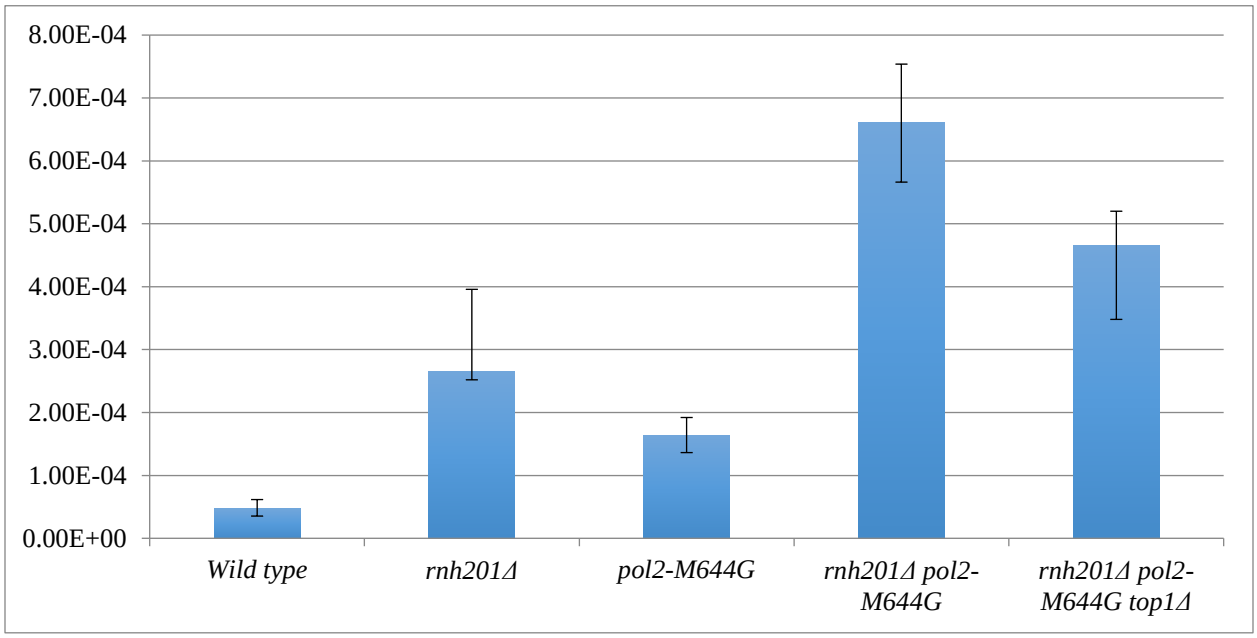

Figure 3. Rates of appearance of 5-FOA-resistant derivatives. The rates of 5-FOA^R derivatives are shown for wild type, *rnh201*Δ, *pol2-M644G*, *rnh201*Δ *pol2-M644G*, and *rnh201*Δ *pol2-M644G top1*Δ strains. The bars indicate the median rates of 5-FOA-resistant derivatives with error bars indicating the 95% confidence intervals. As discussed in the text, this assay monitors the loss of *URA3* by RCO and BIR.

Genome-wide measurements of genome instability using DNA microarrays

The red/white sectoring assay and the assay monitoring loss of *URA3* by the appearance of 5-FOA-resistant derivatives examine genomic instability on the right arm of chromosome IV.

We also used SNP-specific microarrays to look at genomic instability throughout the genome in the *rnh201*Δ, *pol2-M644G*, *rnh201*Δ *pol2-M644G*, and *rnh201*Δ *pol2-M644G top1*Δ strains. This approach is described in detail in St. Charles *et al.* (2012) and in Materials and Methods. In brief, for 13,000 SNPs distributed throughout the genome, we designed four 25-base oligonucleotides per SNP. Two the oligonucleotides are identical to the Watson and Crick strands containing the YJM789-specific SNP, and two are specific for the W303-1A-specific SNP. Under the correct hybridization conditions, genomic DNA from W303-1A hybridizes more strongly to the W303-1A-specific SNP than the YJM789-specific SNP and *vice versa*. This difference allows us to distinguish LOH events as explained in more detail in Materials and Methods.

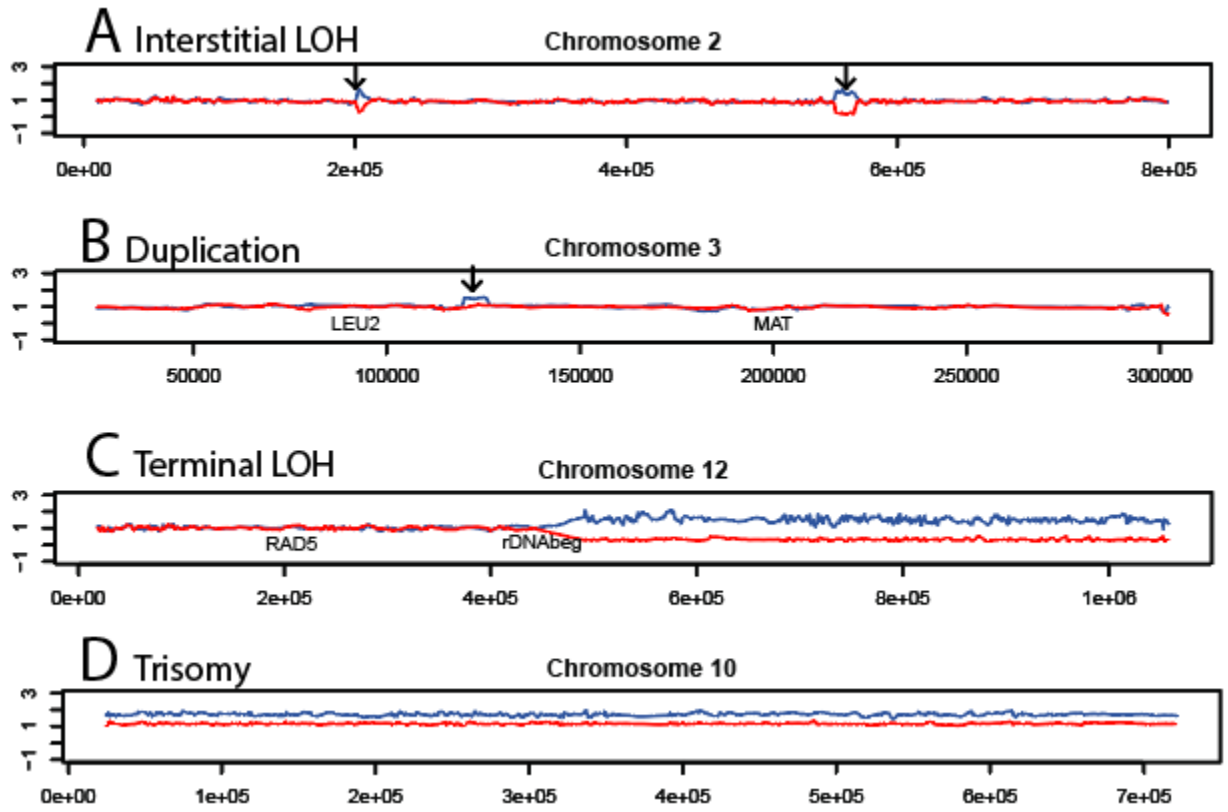

Figure 4. Classes of genome altercations found in sub-cultured strains using microarrays. The y-axis shows the ratio of hybridization of the experimental strain to the control heterozygous strain; the red and blue lines show this ratio to W303-1A- and YJM789-specific SNPs,

respectively. The x-axis shows the Saccharomyces Genome Database coordinate. Events from this image are from an *rnh201*Δ *pol2-M644G top1*Δ strain.

Since the expected number of unselected LOH events was low in the mutant strains, we grew the strains from a single cell to a colony between 10 (about 250 divisions) and 20 (about 500 divisions) times before analyzing the genomic DNA. An example of the microarray analysis for one of the strains is shown in Fig. 4. Among the genetic alterations that we can detect are interstitial LOH events (Fig. 4A), duplication/deletions (Fig. 4B), terminal LOH events, reflecting either RCO or BIR (Fig. 4C), and changes in chromosome number (trisomy event in Fig. 4D). In interstitial LOH events, one region of the chromosome has an elevated hybridization ratio for one homolog and a reduced hybridization ratio for the other; these events are flanked by heterozygous SNPs. Interstitial LOH likely reflects gene conversion, repair of a DSB associated with a non-reciprocal transfer of sequences from one homolog to the other. An event that duplicates SNPs specific to one homolog without deleting SNPs specific to the other homolog are duplications (Fig. 4B). Similarly, heterozygous deletions can be detected as a loss of SNPs from one homolog without a gain of SNPs from the other. In terminal LOH events, a region of LOH extends from an internal site on the chromosome to the chromosome end. Such events could be a consequence of either crossovers or BIR. Lastly, in aneuploidy events, one chromosome is found with a hybridization ratio of about one, and the other chromosome has a hybridization ratio of about 1.5 (trisomy) or 0.2 (monosomy). In my analysis, trisomy was observed, but not monosomy.

The sum of all classes of alterations per genome examined in my study were: 1.36 in *pol2M644G*, 9.76 in *rnh201*Δ *pol2-M644G*, and 5.39 in *rnh201*Δ *pol2-M644G top1*Δ. The comparable numbers for the wild-type and rnh201 strains were 1.4 and 4.95, respectively

(O'Connell *et al.*, 2015). These results, which are displayed in Fig. 5, are broadly consistent with the rates of instability found with the other assays of genome stability.

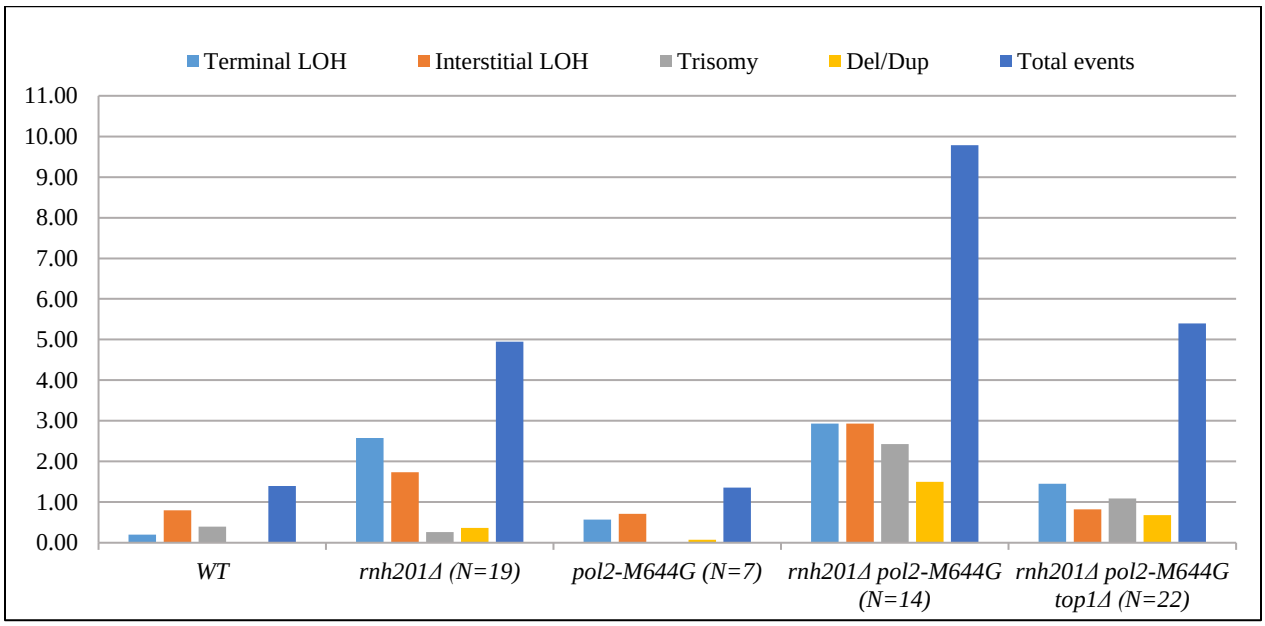

Figure 5. Numbers of genomic alterations in sub-cultured mutant strains. The X-axis shows the number of alterations per sub-cultured strain. The numbers of sub-cultured strains examined for the mutant strains is shown in parentheses after the strain genotype. Ten strains were examined for the wild-type. The total number of genetic alterations per cell in each genotype is shown with the dark blue bar. The wild-type strain was subcultured 10 times, the *rnh201*Δ *pol2-M644G top1*Δ mutant was subcultured 15 times, and all other strains were subcultured 20 times. For this figure, the numbers were normalized as though each strain was sub-cultured 20 times.

In general, these results are in excellent agreement with those obtained by the other two assays. This agreement argues that the observations obtained using assays specific for the right arm of chromosome IV can be generalized to include the whole genome.

Discussion

The results of my analysis of genome stability using three different assays are in Table 1. As in the figures of my thesis, the data for the wild-type and *rnh201* strains are from O'Connell *et al.* (2015). For the red/white sector and 5-FOA-resistance assays, the values shown in the table are the rates of formation of all classes of alterations per cell division on the right arm of chromosome IV. The numbers in parentheses show the rates normalized to a value of 1 for the wild-type strain. The values shown for the whole-genome analysis (bottom row of the table) are the number of genomic alterations of all classes per isolate in sub-cultured strains; as for the other assays, these numbers were normalized to the wild-type value. Since the number of alterations were also normalized to reflect 20 sub-culturings (about 500 cell divisions), I can convert these values to approximate rates of alterations per cell division by dividing the numbers in Table 1 by 500. Thus, the approximate rates of genomic alterations per cell division throughout the genome for the various strains are: wild-type (2.8E-03), *rnh201*Δ (9.9E-03), *pol2-M644G* (2.7E-03), *rnh201*Δ *pol2-M644G* (19E-03), and *rnh201*Δ *pol2-M644G top1*Δ (11E-03). Note that these rates are about ten- to twenty-fold higher than those calculated by the first two assays, as expected, since the first two assays monitor only genomic alterations that occur on the right arm of chromosome IV, and this arm includes about 10% of the total genome.

The three assays are in reasonably good agreement. Relative to the rate of instability in the wild-type strain, the *rnh201*Δ strain had a four- to five-fold elevation. In two of the assays, the *pol2-M644G* strain had a level of instability that was not significantly different from the wild-type strain. Thus, an 11-fold increase in the level of misincorporated rNMPs does not result in elevated genomic instability if the systems that remove the rNMPs (RNase H2 encoded by *RNH201* and Top1) are present. One discrepancy in the assays is that the *pol2-M644G* strain had

a three-fold elevated level of 5-FOA-resistant derivatives compared to the wild-type. One possibility is that 5-fluoro-orotate, in addition to allowing selection for strains that lose the *URA3* gene, also causes a small amount of instability by affecting nucleotide pools (Rossmann *et al.*, 2011). Thus, the data derived from the other two assays, indicating no significant effect of the *pol2-M644G* mutation on genetic instability, are likely more valid

Assays	**Wild-type**	***rnh201Δ***	***pol2-M644G***	***rnh201Δ pol2-M644G***	***rnh201Δ pol2-M644G top1Δ***
Red/White sectors	1.04E-04 (1)	3.73E-04 (3.6)	1.49E-04 (1.4)	1.23E-03 (11.9)	5.35E-04 (5.2)
5-FOA resistance	4.77E-05 (1)	2.66E-04 (5.6)	1.64E-04 (3.4)	6.61E-04 (13.9)	4.66E-04 (9.8)
Whole-genome microarrays	1.40 (1)	4.95 (3.5)	1.36 (1.0)	9.76 (7.0)	5.39 (3.9)

Table 1. Comparison of the levels of genomic instability of wild-type, *rnh201Δ*, *pol2-M644G*, *rnh201Δ pol2-M644G*, and *rnh201Δ pol2-M644G top1Δ* by three different assays. The numeric values in the first two rows are the rates of all classes of genomic alterations per cell division on the right arm of chromosome IV. The values in the last row are the number of alterations throughout the genome per sub-cultured isolate. The values in parentheses show the levels of instability normalized to a value of 1 for the wild-type strain.

Although the *pol2-M644G* mutation has little or no effect on instability as a single mutant, the double *rnh201Δ pol2-M644G* mutant has a level of instability that is two- to three times higher than the single *rnh201*Δ mutant. In addition, the observation that the triple *rnh201*Δ *pol2-M644G top1*Δ mutant has an approximately two-fold reduced level of instability compared to the double mutant indicates that about half of the genetic alterations that occur in the double mutant strain are Top1-dependent. The last important observation that is relevant to my thesis is that strains with the *rnh201*Δ *pol2-M644L* have a level of instability that is only 25% less than the *rnh201*Δ single mutant strain (O'Connell *et al.*, 2015; Conover *et al.*, 2015). The DNA

polymerase encoded by *pol2-M644L* incorporates about three-fold fewer rNMPs than the wild-type polymerase.

As described in the Introduction, *rnh201*Δ strains, which lack functional RNase H2, are expected to have elevated levels of both R-loops and of misincorporated rNMPs. Although several labs have noted that *rnh201*Δ strains have elevated genome instability, different conclusions about the relative contributions of RNA-DNA hybrids and misincorporated rNMPs to the generation of genomic instability were reached. O'Connell *et al.* (2015) suggested that the observation that the *rnh201*Δ *pol2-M644L* strain, which had three-fold fewer rNMPs, had only 25% fewer LOH events argued that RNA-DNA hybrids were a more important cause of instability than rNMPs. If rNMPs were the primary recombinogenic lesion, then one would have expected a reduction of instability by a factor of three in the double mutant strain. Conover *et al.* (2015) emphasized two observations. First, they found that the *pol2-M644G* strain had a seven-fold level of instability compared to wild-type. Second, the *rnh201Δ pol2-M644G* strain had a rate of instability that was about three-fold higher than the *rnh201Δ* single mutant strain. They suggested that these observations implicated misincorporated rNMPs as the primary recombinogenic lesion.

The results of my analysis, as well as those of O'Connell *et al.* and Conover *et al.*, are in substantial agreement, although the interpretations are quite different. The main difference in the data is that Conover *et al.* found that the single mutant *pol2-M644G* had a substantially elevated instability rate, and I found no elevation in instability in two of the three assays that I used. Since Conover *et al.* (2015) used an assay of LOH involving 5-FOA, it is possible (as described above) that their observation is misleading. As I will explain below, the simplest interpretation of all of the studies is that both RNA-DNA hybrids and misincorporated rNMPs can cause genome

instability in different genetic backgrounds. I will discuss the evidence for the recombinogenic effects of these products separately.

Evidence that RNA-DNA hybrids are the primary recombinogenic lesions in rnh201 strains

If we assume that rNMPs are the most important product in generating genetic instability in *rnh201* strains, then the level of instability should be proportional to the number of misincorporated rNMPs. As described above, a three-fold reduction in the number of rNMPs had only a subtle effect on stability (O'Connell *et al.*, 2015). In my analysis, although the *rnh201Δ pol2-M644G* strain had a two- to three-fold elevated increase in instability compared to the *rnh201Δ* strain, the increase was considerably smaller than the 11-fold elevation in the number of rNMPs inserted by the mutant polymerase. Zimmer and Koshland (2016) showed that R-loops were formed at different levels in different regions of chromosome III in *rnh201* strains. Their observation that a region with a high level of R-loops also had a high level of mitotic recombination strongly argues that RNA-DNA hybrids are an important cause of instability in the *rnh201* strain.

Evidence that rNMPs are an important recombinogenic lesion in rnh201Δ pol2-M644G strains

Since the *pol2-M644G* mutation is expected to increase the level of rNMPs, but not affect the level of R-loops, the elevated level of instability observed in the *rnh201Δ pol2-M644G* strain relative to the *rnh201Δ* strain argues that rNMPs can increase genome instability. The reduced instability rates in the *rnh201*Δ *pol2-M644G top1*Δ strain argue that about half of the stimulated events require Top1. The mechanism by which Top1 could produce a DSB is reasonably clear. Top1 would excise the DNA backbone at the rNMP. The linkage formed between Top1 and the

rNMP would be subject to nucleophilic attack by the 2'-OH of the ribose, generating "dirty" 5'-OH and 2',3'-cyclic phosphate ends. These ends must then be processed to allow DNA ligation (Sekiguchi & Shuman, 1997; Williams et al., 2013). If processing is delayed, replication of the intermediate would produce a recombinogenic DSB.

Composite model

To resolve these observations in a single model, I suggest that in the wild-type strain RNA-DNA hybrids are removed by RNase H2 with RNase H1 acting in a backup role. The misincorporated rNMPs are primarily removed by RNase H2 in a mechanism that does not lead to a DNA lesion. Top1 has a minor role in the removal of rNMPs by a mechanism that sometimes results in a DNA nick. Further, I suggest that rNMPs that are not removed are not recombinogenic. Strains with the *pol2-M644G* or *pol2-M644L* have rates of instability similar to wild-type because RNase H2 removes most of the rNMPs by a non-recombinogenic mechanism. If the frequency of misincorporated rNMPs is greatly elevated by the *pol2-M644G* mutation and the efficient removal of rNMPs is prevented by the *rnh201*Δ mutation, then the recombinogenic Top1-associated removal acts on rNMPs, elevating instability.

Conclusion

In closing, I suggest that the genetic stability induced by RNA-DNA hybrids and by rNMPs is a complex function of the frequency with which these intermediates are generated and the way in which these intermediates are repaired by overlapping systems with different properties. A similar conclusion based on other types of evidence has been recently published (Cornelio *et al.*, 2016).

Finally, I should point out that my results are relevant to several human pathologies. Defects in RNA:DNA hybrid maintenance proteins such as RNase H2 have been shown to cause the neurodegenerative disorder, Aicardi-Goutiéres syndrome and is also associated with systemic lupus erythematosus (Crow et al. 2006; Günther et al. 2015). Recent studies have also suggested that particular RNA:DNA hybrids are the triggers for autoimmune disease (Lim et al. 2015).

References Cited:

Aguilera, Andrés, and Tatiana García-Muse. "R loops: from transcription byproducts to threats to genome stability." *Molecular cell* 46.2 (2012): 115-124.

Altman, Douglas G. *Practical statistics for medical research*. CRC press, 1990.

Boeke, Jeffrey, *et al.* "A positive selection for mutants lacking orotidine-5'-phosphate decarboxylase activity in yeast: 5-fluoro-orotic acid resistance." *Mol gen genet* 197.2: 345-346.

Cerritelli, Susana M., and Robert J. Crouch. "Ribonuclease H: the enzymes in eukaryotes." *Febs Journal* 276.6 (2009): 1494-1505.

Clark, Alan B., et al. "Mismatch repair-independent tandem repeat sequence instability resulting from ribonucleotide incorporation by DNA polymerase ε." *DNA repair* 10.5 (2011): 476-482.

Conover, Hailey N., et al. "Stimulation of chromosomal rearrangements by ribonucleotides." *Genetics* 201.3 (2015): 951-961.

Cornelio, Deborah A., et al. "Both R-loop removal and ribonucleotide excision repair activities of RNase H2 contribute substantially to chromosome stability." DNA repair (2017) 52: 110-114.

Costantino, Lorenzo, and Douglas Koshland. "The Yin and Yang of R-loop biology." *Current opinion in cell biology* 34 (2015): 39-45.

Crow, Yanick J., et al. "Mutations in genes encoding ribonuclease H2 subunits cause Aicardi-Goutieres syndrome and mimic congenital viral brain infection." *Nature genetics* 38.8 (2006): 910-916.

Gaillard, Helene, and Andres Aguilera. “Transcription as a Threat to Genome Integrity.” *Ann. review of biochemistry 85* (2016): 291-317.

Günther, Claudia, et al. "Defective removal of ribonucleotides from DNA promotes systemic autoimmunity." *The Journal of clinical investigation* 125.1 (2015): 413-424.

Hamperl, Stephan, and Karlene A. Cimprich. "The contribution of co-transcriptional RNA: DNA hybrid structures to DNA damage and genome instability." *DNA repair* 19 (2014): 84-94.

Huertas, Pablo, and Andrés Aguilera. "Cotranscriptionally formed DNA: RNA hybrids mediate transcription elongation impairment and transcription-associated recombination." *Molecular cell* 12.3 (2003): 711-721.

Joyce, Catherine M. "Choosing the right sugar: how polymerases select a nucleotide substrate." *Proceedings of the National Academy of Sciences* 94.5 (1997): 1619-1622.

Keil, Ralph L., and Roeder, G. Shirleen. “*Cis*-acting, recombination-stimulating activity in a fragment of the ribosomal DNA of *S. cerevisiae*. *Cell 39* (1984): 377-386.

Lea, Douglas E., and Charles Alfred Coulson. "The distribution of the numbers of mutants in bacterial populations." *Journal of genetics* 49.3 (1949): 264.

Lim, Yoong Wearn, et al. "Genome-wide DNA hypomethylation and RNA: DNA hybrid accumulation in Aicardi–Goutieres syndrome." *Elife* 4 (2015): e08007.

McElhinny, Stephanie A. Nick, et al. "Genome instability due to ribonucleotide incorporation into DNA." *Nature chemical biology* 6.10 (2010): 774-781.

Motegi, Akira, and Kyungjae Myung. "Measuring the rate of gross chromosomal rearrangements in Saccharomyces cerevisiae: A practical approach to study genomic rearrangements observed in cancer." *Methods* 41.2 (2007): 168-176.

O’Connell, Karen, Sue Jinks-Robertson, and Thomas D. Petes. "Elevated genome-wide

instability in yeast mutants lacking RNase H activity." *Genetics* 201.3 (2015): 963-975.

Potenski, Catherine J., et al. "Avoidance of ribonucleotide-induced mutations by RNase H2 and Srs2-Exo1 mechanisms." *Nature* 511.7508 (2014): 251-254.

Rossman, Marlies P., *et al.* "A common telomeric gene silencing assay is affected by nucleotide metabolism." *Mol cell* 42.1 (2011): 127-136.

Rydberg, Bjorn, and John Game. "Excision of misincorporated ribonucleotides in DNA by RNase H (type 2) and FEN-1 in cell-free extracts." *Proceedings of the National Academy of Sciences* 99.26 (2002): 16654-16659.

Sparks, Justin L., et al. "RNase H2-initiated ribonucleotide excision repair." *Molecular cell* 47.6 (2012): 980-986.

Sekiguchi, JoAnn, and Stewart Shuman. "Site-specific ribonuclease activity of eukaryotic DNA topoisomerase I." *Molecular cell* 1.1 (1997): 89-97.

St. Charles, Jordan, et al. "High-resolution genome-wide analysis of irradiated (UV and γ-rays) diploid yeast cells reveals a high frequency of genomic loss of heterozygosity (LOH) events." *Genetics* 190.4 (2012): 1267-1284.

Wahba, Lamia, et al. "RNase H and multiple RNA biogenesis factors cooperate to prevent RNA: DNA hybrids from generating genome instability." *Molecular cell* 44.6 (2011): 978-988.

Williams, Jessica S., et al. "Topoisomerase 1-mediated removal of ribonucleotides from nascent leading-strand DNA." *Molecular cell* 49.5 (2013): 1010-1015.

Williams, Jessica S., and Thomas A. Kunkel. "Ribonucleotides in DNA: origins, repair and consequences." *DNA repair* 19 (2014): 27-37.

Williams, Jessica S., et al. "Evidence that processing of ribonucleotides in DNA by

topoisomerase 1 is leading-strand specific." Nature structural & molecular biology 22.4 (2015): 291-297.

Zimmer, Anjali D., and Douglas Koshland. “Differential roles of the RNases H in preventing chromosome instability.” *Proceedings of the National Academy of Sciences* 113.43 (2016): 12220-12225.

Appendix:

Table S1. Genotypes of the diploids analyzed in the study

Strain Name	Relevant genotype	Construction	Complete genotype	Strain Background
KO183	*rnh201Δ pol2-M644G*	KO174 x KO166	*MATa/MATα can1-100/CAN1 TRP1/trp1-1 ade2-1/ade2-1 ura3/ura3-1 LEU2/leu2-3,112 HIS3/his3-11,15 gal2/GAL2 HO/ho::hisG pol2-M644G/pol2-M644G IV1495420::loxP-ADE2-loxP /IV1495420::loxP-K.L.URA3-loxP rnh201Δ::loxP-hph-loxP/rnh201Δ::loxP-hph-loxP*	W303-1A/YJM789
KO184	*pol2-M644G*	KO181 x KO191	*MATa/MATα can1-100/CAN1 trp1-1/TRP1 ade2-1/ade2-1 leu2-3,112/LEU2 his3-11,15/HIS3 ura3-1/ura3 can1-100/CAN1 ho::hisG/ho:hisG GAL2/gal2 IV1495420::loxP-K.L.URA3-loxP/IV1495420::ADE2 pol2-M644G/pol2-M644G*	W303-1A/YJM789
LZ1	*rnh201 pol2-M644G top1Δ*	KO225 x KO277	*MATa/MATα can1-100/CAN1 TRP1/trp1-1 ade2-1/ade2-1 ura3/ura3-1 LEU2/leu2-3,112 HIS3/his3-11,15 gal2/GAL2 HO/ho::hisG pol2-M644G/pol2-M644G IV1495420::loxP-ADE2-loxP /IV1495420::loxP-K.L.URA3-loxP rnh201Δ::loxP-hph-loxP/rnh201Δ::loxP-hph-loxP top1Δ::natMX/top1Δ::natMX*	W303-1A/YJM789

Table S2. Strains utilized in the construction of the diploids analyzed in the study

Strain number	Source	Genotype	Strain background
YJM790	Duke University	*MATa ho::hisG lys2 gal2*	YJM789
SLA42.5	Anderson *et al*., 2015	*MATα ade2-1 ura3 gal2 ho::hisG IV1510386::SUP4-o top1Δ::natMX*	YJM789
SLA36.A	Anderson *et al*., 2015	*MATa leu2-3,112 his3-11,15 ura3-1 ade2-1 trp1-1 can1-100 IV1510386::kanMX top1Δ::natMX pCENTOP1URA3*	W303-1A
SJR3615-4	O'Connell *et al*., 2015	*MATa leu2-3,112 his3-11,15 trp1-1 ura3-1 ade2-1 RAD5 rnh201Δ::loxP-hphMX-loxP IV1510386::kanMX-can1-100*	W303-1A
KO277	Spore of KO221	*MATa ura3-1 ade2-1 trp1-1 can1-100 leu2-3,112 his3-11,15 top1Δ::natMX rnh201Δ::loxP-hphMX-loxP pol2-M644G IV1495420::loxP-K.L.URA3-loxP*	W303-1A
KO225	Spore of KO220	*MATα ho::hisG ade2-1 ura3 gal2 pol2-M644G top1Δ::natMX IV1495420::ADE2 rnh1Δ::loxP-kanMX-loxP rnh201Δ::loxP-hphMX-loxP*	YJM789
KO221	KO195 x KO182	*MATa/MATα ura3-1/ura3-1 ade2-1/ade2-1 trp1-1/trp1-1 can1-100/can1-100 leu2-3,112/leu2-3,112 his3-11,15/his3-11,15 top1Δ::natMX/TOP1 rnh1Δ::loxP-natMX-loxP/RNH1 rnh201Δ::loxP- hphMX-loxP/RNH201 POL2/pol2-M644G IV1495420/IV1495420::loxP-K.L.URA3-loxP*	W303-1A/W303-1A

KO220	KO170 x KO196	*MATa/MATα ho::hisG/ho::hisG ade2-1/ade2-1 ura3/ura3 gal2/gal2 CAN1/can1Δ::natMX pol2-M644G/POL2 TOP1/top1Δ::natMX IV1495420::ADE2/IV1495420 RNH1/rnh1Δ::loxP-kanMX-loxP RNH201/rnh201Δ::loxP-hphMX-loxP pCEN-TOP1-URA3*	YJM789/YJM789
KO196	Spore of KO194	*MATα ade2-1 ura3 ho::hisG top1Δ::natMX rnh1Δ::loxP-kanMX-loxP gal2 rnh201Δ::loxP-hphMX -loxP pCENTOP1-URA3*	YJM789
KO195	Spore of KO193	*MATa leu2-3,112 his3-11,15 ura3-1 ade2-1 trp1-1 can1-100 top1Δ::natMX rnh1Δ::loxP-natMX-loxP rnh201Δ::loxP-hphMX-loxP pCENTOP1URA3*	W303-1A
KO194	KO32 x SLA42.5	*MATa/MATα can1Δ::natMX/CAN1 ade2-1/ade2-1 ura3/ura3 gal2/gal2 ho::hisG/ho::hisG TOP1/top1ΔnatMX IV1510386/IV1510386::SUP4-o rnh1Δ::loxP-kanMX-loxP/RNH1 rnh201Δ::loxP-hphMX-loxP/RNH201 pCEN-TOP1-URA3*	YJM789/YJM789
KO193	KO63 x SLA36.A	*MATa/MATα leu2-3,112/leu2-3,112 his3-11,15/his3-11,15 ura3-1/ura3-1 ade2-1/ade2-1 trp1-1/trp1-1 can1-100/can1-100 IV1510386::kanMX/IV1510386 top1Δ::natMX/TOP1 RNH1/rnh1Δ::loxP-natMX-loxP RNH201/rnh201Δ::loxP-hphMX-loxP pCENTOP1URA3*	W303-1A/W303-1A
KO192	KO171 x KO157	*MATa/MATα can1-100/CAN1 trp1-1/trp1-1 ade2-1/ade2-1 leu2-3,112/leu2-3,112 his3-11,15/his3-11,15 ura3-1/ura3-1*	W303-1A/W303-1A

		POL2/pol2-M644G IV1495420::loxP-K.L.URA3-loxP/IV1495420 RNH201/rnh201::loxP-hphMX-loxP RNH1/rnh1::loxP-natMX-loxP	
KO191	Spore of KO163	*MATα ho::hisG gal2 ura3 IV1495420::ADE2 pol2-M644G ade2-1*	W303-1A/YJM789
KO182	Spore of KO192	*MATα ade2-1 ura3-1 leu2-3,112 his3-11,5 can1-100 ho::hisG pol2-M644G IV1495420::loxP-K.L.URA3-loxP*	W303-1A
KO181	Spore of KO192	*MATa can1-100 trp1-1 ade2-1 ura3-1 leu2-3,112 his3-11,15 IV1495420::loxP-K.LactisURA3-loxP pol2-M644G*	W303-1A
KO174	Spore of KO192	*MATα trp1-1 ura3-1 ade2-1 leu2-3,112 his3-11,15 can1-100 pol2-M644G rnh201Δ::loxP-hph-loxP IV1495420::loxP-K.L.URA3-loxP*	W303-1A
KO171	O'Connell *et al*., 2015	*MATa can1-100 trp1-1 ade2-1 his3-11,15 leu2-3,112 ura3Δ::loxP-kanMX-loxP IV1495420::loxP-URA3K.L.-loxP*	W303-1A
KO170	Spore of KO163	*MATa ho::hisG gal2 ura3 ade2-1 can1Δ::natMX IV1492420::ADE2 pol2-M644G*	YJM789
KO166	Spore of KO163	*MATa ho::hisG ura3 gal2 ade2-1 CAN1 IV1495420::ADE2 pol2-M644G rnh201Δ::loxP-HPH-loxP*	YJM789
KO163	KO162xKO33_1	*MATa/MATα ho::hisG/ho::hisG gal2/gal2 ura3/ura3 ade2Δ::kanMX/ade2-1 CAN1/can1 Δ::natMX IV1495420::ADE2/IV1495420*	YJM789

		RNH1/rnh1Δ::loxP-kanMX-loxP RNH201/rnh201Δ::loxP-hphMX-loxP pol2-M644G/POL2	
KO162	Spore of KO161	*MATa ho::hisG gal2 ura3 ade2Δ::kanMX IV1495420::ADE2 pol2-M644G*	YJM789
KO161	KO153 x YJM790	*MATa/MATα ho::hisG/ho::hisG lys2/LYS2 gal2/gal2 URA3/ura3 ADE2/ade2Δ::kanMX IV1495420/IV1495420::ADE2 POL2/pol2-M644G*	YJM790/YJM789
KO160	KO152 x SJR3615-4	*MATa/MATα leu2-3,112/leu2-3,112 ura3-1/ura3-1 his3-11,15/his3-11,15 trp1-1/trp1-1 ade2-1/ade2-1 IV1510386::kanMX-can1-100/IV1510386 RNH1/rnh1Δ::loxP-nat-loxP rnh201Δ::loxP-HPH-loxP/RNH201 POL2/pol2-M644G*	W303-1A/W303-1A
KO157	Spore of KO160	*MATα leu2-3, 112 his3-11,15 trp1-1 ura3-1 ade2-1 rnh201Δ::loxP-HPH-loxP pol2-M644G*	W303-1A
KO153	KO124 after a two-step allele replacement using plasmid pSR1007-pol2-M644G after digestion with AgeI	*MATalpha ura3 gal2 ho::hisG ade2Δ::kanMX IV1495420::ADE2 pol2-M644G*	YJM789
KO152	KO67 after a two-step allele replacement using plasmid pSR1007-pol2-M644G after digestion with AgeI	*MATα leu2-3,112 his3-11,15 trp1-1 ura3-1 ade2-1 pol2-M644G rnh1Δ::loxP-nat-loxP*	W303-1A

KO124	O'Connell *et al.*, 2015	*MATα ade2Δ::kanMX ura3 ho::hisG gal2 IV1495420::ADE2*	YJM789
KO67	Spore of KO52	*MATα leu2-3,112 his3-11,15 trp1-1 ura3-1 ade2-1 rnh1Δ::loxP-nat-loxP*	W303-1A
KO63	Spore of KO52	*MATα leu2-3,112 his3-11,15 trp1-1 ura3-1 ade2-1 can1-100 IV1510386 rnh1Δ::loxP-natMX-loxP rnh201Δ::loxP-hphMX-loxP*	W303-1A
KO52	O'Connell *et al.*, 2015	*MATa/MATα leu2-3,112/leu2-3,112 his3-11,15/his3-11,15 trp1-1/trp1-1 ura3-1/ura3-1 ade2-1/ade2-1 CAN1/can1-100 IV1510386::kanMX-can1-100/IV1510386 rnh1Δ::loxP-natMX-loxP/RNH1 rnh201Δ::loxP-hphMX-loxP/RNH201*	W303-1A/W303-1A
KO32	O'Connell *et al.*, 2015	*MATa can1Δ::natMX ade2-1 ura3 ho::hisG gal2 rnh1Δ::loxP-kanMX-loxP rnh201Δ::loxP-hphMX-loxP*	YJM789